Int. J. Heat Mass Transfer. Vol. 33, No. 12, pp. 2615–2623, 1990
Printed in Great Britain

0017–9310/90 $3.00 + 0.00

Transition from subcritical to supercritical bifurcation in penetrative convection in a vertical cylinder

CHRISTIANE NORMAND

Service de Physique Theorique (Laboratoire de l'Institut de Recherche Fondamentale du Commissariat à l'Energie Atomique), C.E.N. Saclay, F-91 191, Gif-sur-Yvette Cedex, France

(*Received* 7 *June* 1989 *and in final form* 2 *February* 1990)

Abstract—The stability of a vertical cylindrical column of water with the horizontal bottom boundary maintained at 0°C and the temperature of the top boundary varying between 4 and 8°C is considered. A weakly non-linear analysis shows that the bifurcation is either supercritical or subcritical depending upon the values of two parameters: the aspect ratio of the cylinder (height/radius) which is varied between 2 and 4, and the penetration parameter μ defined as the ratio of the whole height over the height of the 4°C isotherm. For a given value of the aspect ratio, the bifurcation is supercritical when the whole height is unstable ($\mu = 1$) and becomes subcritical above a particular value of μ when penetration occurs ($\mu > 1$).

1. INTRODUCTION

PENETRATIVE convection occurs when an unstably stratified layer of fluid is bounded either above or below by a stably stratified layer. This arises when considering the melting of an ice layer or the freezing of a water layer. Because of the density maximum of water near 4°C, the water below the 4°C isotherm is unstable. The onset of convection in a horizontal water layer near its density extremum has been widely studied. Veronis [1] considered the temperature range from 0 to 8°C where the equation of state is accurately approximated by a parabolic density–temperature relation. Merker *et al.* [2] assuming a fifth-order polynomial for the density–temperature relation showed that the critical Rayleigh numbers calculated with the simple parabolic relation are about 10% too large. Gebhart and Mollendorf [3] have also developed a density–temperature relation valid for both pure and saline water.

Thermal instability in a fluid with a non-linear density profile arises in many fields of geophysical fluid dynamics. It takes place in the earth's mantle, its atmosphere, lakes and oceans. It also occurs in the outer layer of the sun. Recently, as a model of penetrative convection appropriate to geophysical applications, Matthews [4] analysed the stability of a cubic temperature profile. He showed, using a weakly non-linear analysis, that the bifurcation is supercritical, this result being in contrast with the subcritical bifurcation found earlier by Veronis [1] for water between 0 and 8°C. This leads him to distinguish between a non-linear density profile produced by a non-linear equation of state with a linear temperature profile, and a non-linear density profile produced by a linear equation of state with a non-linear temperature profile. However, this difference cannot be a sufficient criterion to determine a priori the nature of the bifurcation.

Transition to finite amplitude convection also appears as a result of numerical calculations achieved for the ice–water system confined between free upper and lower surfaces of infinite horizontal extent [5, 6]. When the fluid is bounded by no-slip horizontal surfaces with a fixed-heat-flux thermal boundary condition, Roberts [7] has shown that simplifications occur in the analytical treatment enabling predictions to be made about the extent of subcriticality.

An hysteretic transition near the critical Rayleigh number has been observed in experiments with liquid helium which has a density maximum just above the superfluid transition temperature [8].

The aim of the present analysis is to reconsider the ice–water system where a subcritical bifurcation is expected for water between 0 and 8°C [1]. By varying the temperature of the horizontal top boundary from 4 to 8°C it will be shown that the bifurcation can be either supercritical or subcritical following the relative height of the unstable layer. We have considered a vertical cylindrical column of water because experiments have already been performed in this geometry [9, 10] and to see how finite size effects affect the nature of the bifurcation. Moreover, in this geometry the horizontal structure of the convective flow can be considerably simplified by a suitable choice of the lateral vertical boundary conditions that determine the horizontal wave numbers (radial and azimuthal). Therefore, in determining the onset of convection we avoid minimization of the Rayleigh number with respect to the horizontal wave number.

2. FORMULATION OF THE PROBLEM

Consider a vertical cylinder of radius R and height h filled with water. The top and bottom horizontal

NOMENCLATURE

a_{ni}	integral of product of three Bessel functions
d	height of maximum density
d_{ni}	coefficients in the denominator of the expression for R_2
D	derivative with respect to the vertical variable, d/dz
e	unit vector in the upward vertical direction
F	combination of the double products of Bessel functions
g	acceleration due to gravity
h	height of the cylinder
p	convective pressure
J_n	Bessel function of order n
k	radial wave number
n	angular wave number
r, φ, z	cylindrical polar coordinates (radial, azimuthal, vertical)
R	radius of the cylinder
Ra	Rayleigh number
$Ra^{(n,i)}$	critical Rayleigh number of the nth azimuthal mode and ith vertical mode
R_2	second term in the ε-expansion of the Rayleigh number
$R_{2j}^{(i)}$	coefficients in the polynomial expansion of R_2 in inverse power of the Prandtl number, $j = 1, 3$
t	time
T	temperature
T_0, T_1	temperature at the bottom and the top of the cylinder
T_m	temperature of maximum density
ΔT	temperature difference between T_m and T_0
$\mathbf{u}$	convective velocity, (u, v, w)
$\mathbf{U}_n$	nth term in the perturbative expansion of velocity
x	new variable proportional to the radial variable
X, X^*	vertical profile of the temperature and its adjoint
Y, Y^*	vertical profile of the velocity potential and its adjoint
Z	Laplacian of Y.

Greek symbols

$\alpha_n^{(i)}, \alpha_{nj}^{(i)}$	volume integrals of the non-linear terms, $j = 1, 3$
β	thermal expansion coefficient
δ	differential operator
Δ_H	horizontal Laplacian
ε	expansion parameter
θ	convective temperature
Θ_n	nth term in the expansion of θ
κ	thermal diffusivity
λ	aspect ratio of the cylinder, h/R
μ	penetration parameter, h/d
ν	kinematic viscosity
σ	Prandtl number, ν/κ
ϕ	velocity potential
Φ_n	nth term in the expansion of ϕ
$\Omega(z)$	linear function of z.

Other symbol

∇	gradient.

boundaries are held at different temperatures, T_1 and T_0. The physical situation to be described corresponds to $T_0 = 0°C$ and $8°C \geqslant T_1 \geqslant T_m$. In this range of temperature the viscosity ν and the thermal diffusivity κ are assumed to be constant. The density ρ is a quadratic function of the temperature

$$\rho = \rho_m[1-\beta(T-T_m)^2].$$

The temperature T_m for which the density maximum occurs is located at a height d with $0 < d < h$. Then the temperature distribution in the conductive state is

$$T = T_0+(T_m-T_0)\frac{z}{d}, \quad 0 < z < h. \tag{1}$$

Also we shall denote by ΔT the temperature difference $T_m - T_0$. In a vertical cylinder it is convenient to use R as a length scale and $\Delta T(R/d)$ as a temperature scale. Nondimensionalizing the velocity with κ/R and the time with R^2/κ, the equations for the perturbed velocity $\mathbf{u} = (u, v, w)$, pressure p and temperature θ become

$$\frac{1}{\sigma}\left(\frac{\partial \mathbf{u}}{\partial t}+\mathbf{u}\cdot\nabla\mathbf{u}\right) = -\nabla p + Ra\left(\frac{\mu}{\lambda}z-1\right)\theta\mathbf{e}+\nabla^2\mathbf{u} \tag{2}$$

$$\left(\frac{\partial \theta}{\partial t}+\mathbf{u}\cdot\nabla\theta\right) = \nabla^2\theta - w \tag{3}$$

where $\mathbf{e}$ is the unit vector in the upward z-direction, $\sigma = \nu/\kappa$ is the Prandtl number and Ra the Rayleigh number given by

$$Ra = \frac{2\beta g \Delta T^2 R^4}{\nu\kappa d}. \tag{4}$$

In the definition above the Rayleigh number is constructed with the height of the unstable part [1] rather than with the height of the cylinder [2]. Due to the finite geometry and the density anomaly, two other

parameters are required to describe the convective state : the aspect ratio $\lambda = h/R$ and $\mu = h/d$.

We assume that the top and bottom horizontal boundaries are isothermal and rigid surfaces, leading to the boundary conditions

$$\theta = u = v = w = 0 \text{ on } z = 0, \lambda, \quad 0 \leqslant r < 1. \quad (5)$$

The lateral boundary is assumed to be a perfectly insulating surface on which the tangential vorticity is zero. The resulting boundary conditions are

$$\frac{\partial \theta}{\partial r} = u = \frac{\partial (rv)}{\partial r} = \frac{\partial w}{\partial r} = 0 \text{ on } r = 1, \quad 0 < z < \lambda. \quad (6)$$

Following Rosenblat [11] these boundary conditions have been chosen in order to simplify the mathematical analysis and they seem satisfactory to provide a qualitative interpretation of the realistic physical behaviour.

3. LINEAR STABILITY

Assuming the validity of the principle of exchange of stabilities, the linearization of system (2) and (3) is obtained by setting the right-hand sides equal to zero. As a result we obtain

$$0 = -\nabla p + Ra\left(\frac{\mu}{\lambda} z - 1\right)\theta \mathbf{e} + \nabla^2 \mathbf{u} \quad (7)$$

$$0 = \nabla^2 \theta - w. \quad (8)$$

Boundary conditions (6) allow the search for solutions with no vertical vorticity. Thus we introduce the velocity potential ϕ such that $\mathbf{u} = \nabla \times \nabla \times \phi \mathbf{e}$. Moreover, separation of variables is possible and we put

$$\phi(r, \varphi, z) = \cos n\varphi \, J_n(kr) \, Y(z) \quad (9)$$

$$\theta(r, \varphi, z) = \cos n\varphi \, J_n(kr) X(z) \quad (10)$$

where $n = 0, 1, 2, \ldots$ is the azimuthal wave number, J_n the Bessel function of order n, and k is determined from the equation $J_n'(k) = 0$. Since we are interested in cylinders with an aspect ratio $\lambda > 1$ the radial structure of the critical mode is expected to be that corresponding to the first positive zero of J_n', as it occurs when convection takes place in the whole height.

Acting with $\mathbf{e} \cdot \nabla \times \nabla \times$ on equation (7) the system (7) and (8) reduces to a pair of ordinary differential equations

$$(D^2 - k^2)^2 Y - Ra\left(\frac{\mu}{\lambda} z - 1\right) X = 0 \quad (11)$$

$$(D^2 - k^2) X - k^2 Y = 0 \quad (12)$$

subject to the boundary conditions

$$Y = DY = X = 0 \quad \text{at} \quad z = 0, \lambda \quad (13)$$

where $D = d/dz$. The system of equations (11)–(13) was integrated numerically using a fourth-order Runge–Kutta method which was described in a previous paper [10]. Non-trivial solutions exist for certain values of the Rayleigh number $Ra^{(n,i)}$, where n characterizes the horizontal structure (both azimuthal and radial) and i the vertical structure. The results for different values of μ and λ (Tables 1–3), show that the critical mode always corresponds to an azimuthal number $n = 1$ associated with a radial wave number $k_1 = 1.841$. The vertical structure of the critical mode ($i = 1$) is made of one principal cell with sometimes a small counter cell in the upper part of the cylinder when $\mu > 1.5$ (Figs. 1 and 2). To each eigenvalue $Ra^{(n,i)}$ corresponds an eigenvector (Y_{ni}, X_{ni}) and consequently the three components of velocity and temperature are written as follows:

$$u_{ni} = k_n \cos n\varphi \, J_n'(k_n r) D Y_{ni}(z)$$

$$v_{ni} = -n \sin n\varphi \, J_n(k_n r) D Y_{ni}(z)$$

$$w_{ni} = k_n^2 \cos n\varphi \, J_n(k_n r) Y_{ni}(z)$$

$$\theta_{ni} = \cos n\varphi \, J_n(k_n r) X_{ni}(z).$$

It has already been shown [10] that for large values of the aspect ratio ($\lambda \to \infty$), an asymptotic form of the vertical profiles $Y_{ni}(z)$ and $X_{ni}(z)$ can be found in terms of Airy functions.

Table 1. Critical values of the Rayleigh number $Ra^{(n,i)}$ as a function of μ for the angular modes $n = 1, 2, 0$ and the first three vertical modes $i = 1, 2, 3$. The value of the aspect ratio is $\lambda = 2$

μ	i	$Ra^{(1,i)}$	$Ra^{(2,i)}$	$Ra^{(0,i)}$
1	1	110.26	216.63	376.03
	2		1233.44	1461.13
	3		5730.88	5401.98
1.1	1	121.95	237.93	410.17
	2		1427.89	1686.84
	3		6863.81	6460.05
1.2	1	136.26	263.18	449.51
	2		1702.72	1996.33
	3		8739.01	8157.36
2	1	588.38	748.61	1049.78
	2		12976.58	11566.75

Table 2. Critical values of the Rayleigh number $Ra^{(n,i)}$ as a function of μ for the angular modes $n = 1, 2, 0$ and the first three vertical modes $i = 1, 2, 3$. The value of the aspect ratio is $\lambda = 3$

μ	i	$Ra^{(1,i)}$	$Ra^{(2,i)}$	$Ra^{(0,i)}$
1	1	35.03	123.86	253.05
	2		370.54	583.39
	3		1126.32	1391.42
1.2	1	42.77	145.54	290.00
	2		499.27	763.82
	3		1681.11	2027.81
1.4	1	54.09	172.60	333.02
	2		720.99	1031.91
	3		2933.93	3226.49
2	1	133.08	295.55	507.66
	2		2287.60	2611.31

Table 3. Critical values of the Rayleigh number $Ra^{(n,i)}$ as a function of μ for the angular modes $n = 1, 2, 0$ and the first three vertical modes $i = 1, 2, 3$. The value of the aspect ratio is $\lambda = 4$

μ	i	$Ra^{(1,i)}$	$Ra^{(2,i)}$	$Ra^{(0,i)}$
1	1	21.14	97.86	211.40
	2		213.28	389.87
	3		479.06	722.62
1.2	1	25.36	111.39	235.01
	2		276.50	484.69
	3		692.01	999.37
1.4	1	31.04	126.91	261.02
	2		367.05	606.41
	3		1073.88	1419.73
1.6	1	38.62	144.69	289.76
	2		490.32	760.68
	3		1663.25	2020.55
1.8	1	48.55	165.06	321.63
	2		655.97	956.29
	3		2552.89	2872.74
2	1	61.25	188.47	357.06
	2		878.10	1204.42
	3		3871.32	4070.27

4. NON-LINEAR ANALYSIS

When the solutions of the linear problem cannot be expressed in terms of analytical functions, the non-linear problem can always be solved by a standard perturbation method. Nevertheless a Galerkin procedure is sometimes preferred [11]. The selection of a minimal set of modes as a basis of the expansion in the Galerkin formulation is rather arbitrary and we choose to present the perturbation method, though in our case both methods give identical results. The unknown functions are expanded in power series as

$$\mathbf{u} = \varepsilon \mathbf{U}_1 + \varepsilon^2 \mathbf{U}_2 + \varepsilon^3 \mathbf{U}_3 + \cdots \tag{14}$$

$$\theta = \varepsilon \Theta_1 + \varepsilon^2 \Theta_2 + \varepsilon^3 \Theta_3 + \cdots \tag{15}$$

$$\phi = \varepsilon \Phi_1 + \varepsilon^2 \Phi_2 + \varepsilon^3 \Phi_3 + \cdots \tag{16}$$

$$Ra = Ra^{(1,1)} + \varepsilon^2 R_2 + \varepsilon^4 R_4 + \cdots \tag{17}$$

where $\mathbf{U}_1 = (u_{11}, v_{11}, w_{11})$ and $\Theta_1 = \theta_{11}$ are solutions of the linear problem corresponding to the critical Rayleigh number $Ra^{(1,1)}$. In the Rayleigh number expansion the term proportional to ε has been omitted

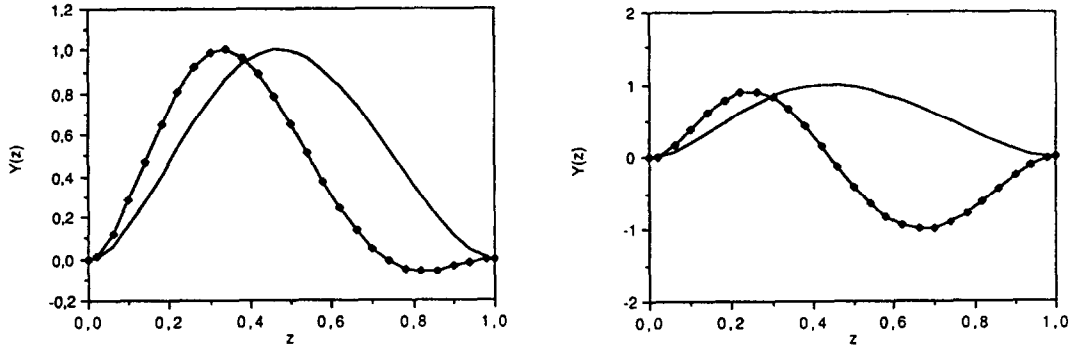

FIG. 1. Eigenfunctions $Y_{ni}(z)$ for the aspect ratio $\lambda = 2$. (a) $n = 1$, $i = 1$: ——, $\mu = 1$; —◆—, $\mu = 2$. (b) $\mu = 1$: ——, $n = 2$, $i = 1$; —◆—, $n = 2$, $i = 2$.

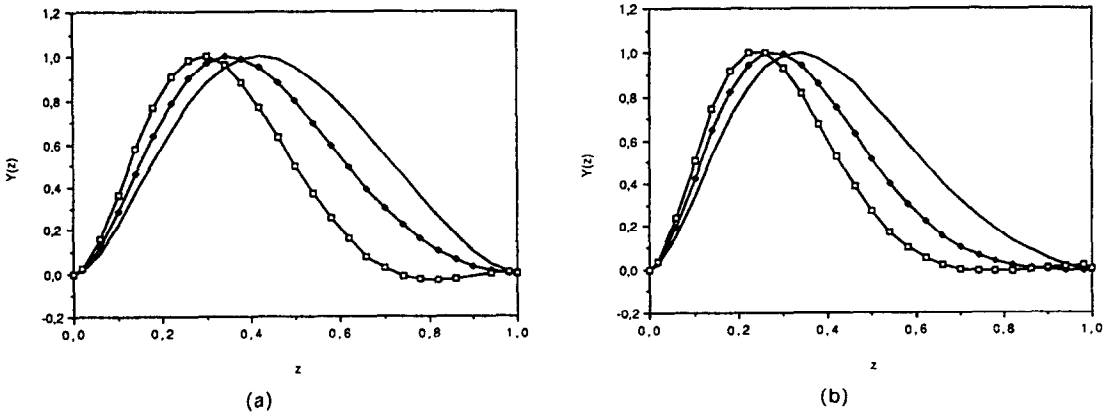

FIG. 2. Eigenfunctions $Y_{n1}(z)$ for the aspect ratio $\lambda = 4$. (a) $n = 1$: ——, $\mu = 1$; —◆—, $\mu = 1.5$; —○—, $\mu = 2$. (b) $n = 2$: ——, $\mu = 1$; —◆—, $\mu = 1.5$; —○—, $\mu = 2$.

because a transcritical bifurcation is excluded when the critical mode is the diametrically antisymmetrical one ($n = 1$). In Marangoni convection Rosenblat *et al.* [12] have shown that a transcritical bifurcation is expected when the critical mode is the axisymmetrical one ($n = 0$). In cylindrical geometry, the angular mode $n = 0$ has the same behaviour as the hexagonal pattern in an infinite horizontal layer. A summary of the principal types of bifurcation can be found in the paper by Benjamin [13]. The expansions above, equations (14)–(17), are substituted into the non-linear system

$$\frac{1}{\sigma}\delta\cdot(\mathbf{u}\cdot\nabla)\mathbf{u} = \nabla^4\Delta_H\phi - Ra\left(\frac{\mu}{\lambda}z-1\right)\Delta_H\theta \quad (18)$$

$$\mathbf{u}\cdot\nabla\theta = \nabla^2\theta - w \quad (19)$$

obtained from equations (2) and (3) by taking $\mathbf{e}\cdot(\nabla\times\nabla\times)$ of equation (2) and where $\delta = \nabla\times\nabla\times\mathbf{e}$. For each equation the coefficient of each power of ε must vanish. At second order this gives

$$\frac{1}{\sigma}\delta\cdot(\mathbf{U}_1\cdot\nabla)\mathbf{U}_1 = \nabla^4\Delta_H\Phi_2 - Ra^{(1,1)}\left(\frac{\mu}{\lambda}z-1\right)\Delta_H\Theta_2 \quad (20)$$

$$\mathbf{U}_1\cdot\nabla\Theta_1 = \nabla^2\Theta_2 + \Delta_H\Phi_2 \quad (21)$$

where Δ_H is the horizontal Laplacian in polar coordinates

$$\Delta_H = \frac{1}{r}\frac{\partial}{\partial r}r\frac{\partial}{\partial r} + \frac{1}{r^2}\frac{\partial^2}{\partial\varphi^2}. \quad (22)$$

Explicit expressions of the non-linear terms on the left-hand side of equations (20) and (21) are given in the Appendix. They are composed of two different azimuthal contributions corresponding respectively to the angular modes $n = 0$ and 2. This suggests the need to look for approximate solutions of equations (20) and (21) in the form

$$\Phi_2 = \cos 2\varphi\, J_2(k_2 r)\sum_{i=1}^{N} A_{2i}Y_{2i}(z) + J_0(k_0 r)\sum_{i=1}^{N} A_{0i}(z)\,Y_{0i}(z) \quad (23)$$

$$\Theta_2 = \cos 2\varphi\, J_2(k_2 r)\sum_{i=1}^{N} A_{2i}X_{2i}(z) + J_0(k_0 r)\sum_{i=1}^{N} A_{0i}X_{0i}(z) \quad (24)$$

with $k_2 = 3.054$ and $k_0 = 3.832$.

The coefficients A_{2i} and A_{0i} are determined using a Galerkin procedure and at this stage of the calculation the perturbative expansion technique becomes equivalent to a Galerkin method with the set of selected modes

$$S = \{11, 2i, 0i\}, \quad i = 1,\ldots,N.$$

Using symmetry arguments it is sometimes possible to reduce the number of vertical modes to either $i = 2$ [11] or 1 [12]. In the present case it will be shown that at least two modes are necessary to get accurate results.

Since the linear problem (11)–(13) is not selfadjoint we need the solutions Y^*_{ni} and X^*_{ni} of the adjoint problem

$$(D^2-k^2)^2Y^* + X^* = 0 \quad (25)$$

$$(D^2-k^2)X^* + Rak^2\left(\frac{\mu}{\lambda}z-1\right)Y^* = 0 \quad (26)$$

$$Y^* = DY^* = X^* = 0 \quad \text{at} \quad z = 0,\lambda. \quad (27)$$

This system is integrated numerically using a Runge–Kutta method. Multiplying equations (20) and (21) by the adjoint eigenfunctions $(\phi^*_{ni}, \theta^*_{ni})$ for respectively $n = 0, 2$ and integrating over the volume of the cylinder we find that

$$-k_n^2 d_{ni}(Ra^{(n,i)} - Ra^{(1,1)})A_{ni} = \left\langle \frac{1}{\sigma}\phi^*_{ni}\delta\cdot(\mathbf{U}_1\cdot\nabla)\mathbf{U}_1 + \theta^*_{ni}(\mathbf{U}_1\cdot\nabla)\Theta_1 \right\rangle \quad (28)$$

where

$$d_{ni} = \langle\phi^*_{ni}\Omega(z)\theta_{ni}\rangle. \quad (29)$$

To simplify we have introduced the notation $\Omega(z) = (\mu z/\lambda - 1)$. The angular brackets denote integration over the volume $0 \leqslant r < 1$, $0 < \varphi < 2\pi$, $0 < z < \lambda$. It is convenient to introduce the following quantities:

$$\alpha^{(i)}_{n1} = \left\langle \frac{1}{\sigma}\phi^*_{ni}\delta\cdot(\mathbf{u}_{11}\cdot\nabla)\mathbf{u}_{11} + \theta^*_{ni}(\mathbf{u}_{11}\cdot\nabla)\theta_{11} \right\rangle, \quad n = 0,2, \quad i = 1,\ldots,N \quad (30)$$

which involve calculation of radial and vertical integrals reported in the Appendix.

At third order in ε, the equations are

$$\frac{1}{\sigma}\delta\cdot[(\mathbf{U}_1\cdot\nabla)\mathbf{U}_2 + (\mathbf{U}_2\cdot\nabla)\mathbf{U}_1] + R_2\Omega(z)\Delta_H\Theta_1 = \nabla^4\Delta_H\Phi_3 - Ra^{(1,1)}\Omega(z)\Delta_H\Theta_3 \quad (31)$$

$$(\mathbf{U}_1\cdot\nabla)\Theta_2 + (\mathbf{U}_2\cdot\nabla)\Theta_1 = \nabla^2\Theta_3 + \Delta_H\Phi_3. \quad (32)$$

The solvability conditions leads to the following expression for R_2:

$$k_1^2 d_{11}R_2 = \frac{1}{\sigma}\langle\phi^*_{11}\delta\cdot[(\mathbf{U}_1\cdot\nabla)\mathbf{U}_2 + (\mathbf{U}_2\cdot\nabla)\mathbf{U}_1]\rangle + \langle\theta^*_{11}[(\mathbf{U}_1\cdot\nabla)\Theta_2 + (\mathbf{U}_2\cdot\nabla)\Theta_1]\rangle \quad (33)$$

or

$$k_1^2 d_{11}R_2 = \sum_{i=1}^{N} A_{0i}\alpha_0^{(i)} + \sum_{i=1}^{N} A_{2i}\alpha_2^{(i)} \quad (34)$$

where

$$\alpha_n^{(i)} = \frac{1}{\sigma}\langle\phi^*_{11}\delta\cdot[(\mathbf{u}_{11}\cdot\nabla)\mathbf{u}_{ni} + (\mathbf{u}_{ni}\cdot\nabla)\mathbf{u}_{11}]\rangle + \langle\theta^*_{11}[(\mathbf{u}_{11}\cdot\nabla)\theta_{ni} + (\mathbf{u}_{ni}\cdot\nabla)\theta_{11}]\rangle, \quad n = 0,2 \quad (35)$$

factorizes in radial and vertical integrals as shown in the Appendix. Finally R_2 is expressed as the sum of N contributions

$$R_2 = -\frac{1}{k_1^2 d_{11}} \sum_{i=1}^{N} \frac{1}{d_{0i} k_0^2} \frac{\alpha_0^{(i)} \alpha_{01}^{(i)}}{(Ra^{(0,i)} - Ra^{(1,1)})} + \frac{1}{k_2^2 d_{2i}} \frac{\alpha_0^{(i)} \alpha_{01}^{(i)}}{(Ra^{(0,i)} - Ra^{(1,1)})} \quad (36)$$

Similar expressions have been derived previously also for fluid in a circular cylinder but with different symmetrical properties than in the present case. Rosenblat [11] considered ordinary liquid with a linear state equation and free upper and lower horizontal surfaces. In this physical situation it can be shown that: $\alpha_n^{(1)} = \alpha_{n1}^{(1)} = 0$, $\alpha_n^{(2)} = -\alpha_{n1}^{(2)}$ $(n = 0, 2)$ as mentioned in the Appendix. Since $Ra^{(n,i)} > Ra^{(1,1)}$ and $d_{ni} > 0$ it was found that $R_2 > 0$ leads to a supercritical bifurcation. This is the expected result when reflection symmetry with respect to the mid-height is present. Rosenblat *et al.* [12] examined also the case of Marangoni convection where the reflection symmetry is broken but they conclude that even in that case the bifurcation is supercritical for all Prandtl numbers. The principal difference with the present analysis is that previous works dealt with the case of moderate aspect ratio ($R > h$) while we are dealing with the opposite limit ($h > R$). Therefore, in the Galerkin formulation they considered a minimal set of modes with an elementary vertical structure corresponding to $i = 1$ in the non-symmetrical case or $i = 2$ in the symmetrical case. Here we need to consider both the contributions due to $i = 1$ and 2. This is partially due to the fact that when the aspect ratio increases, the Rayleigh numbers at which two successive vertical modes destabilize become closer (Tables 1–3) and the term $(Ra^{(n,i)} - Ra^{(1,1)})$ in the denominator of expression (37) can no longer act as a damping factor when $i > 1$. When there is no reflection symmetry and for moderate aspect ratio Rosenblat *et al.* [12] calculated the contribution to R_2 due to the first excited vertical mode ($i = 1$) and neglected the contribution of modes $i \geqslant 2$. For large aspect ratio this approximation fails and we will see in the next section that the contribution due to $i = 2$ is greater than that due to $i = 1$.

5. NATURE OF THE BIFURCATION

In this section we present the results of the calculation of R_2 for three specific values of the aspect ratio $\lambda = 2, 3, 4$. We can write R_2 as a function of the Prandtl number σ

$$R_2 = \sum_{i=1}^{2} R_{20}^{(i)} + \frac{1}{\sigma} R_{21}^{(i)} + \frac{1}{\sigma^2} R_{22}^{(i)}. \quad (37)$$

5.1. *Bifurcation at* $\lambda = 2$

Inspection of Table 4 where the values of $R_{20}^{(i)}$, $R_{21}^{(i)}$ and $R_{22}^{(i)}$ have been reported shows that the coefficients $R_{21}^{(i)}$ take positive values and that the contribution corresponding to $i = 2$ is larger than that corresponding to $i = 1$ for small values of μ while the contrary is true for $\mu > 1.5$. The contribution of the third vertical mode ($i = 3$) being an order of magnitude lower than the leading one will not be considered in the following. The major contribution to $R_{22}^{(i)}$ comes from $i = 2$, the smaller contributions from $i = 1$ and 3 being nearly equal and of opposite sign. On Fig. 1 we have drawn the function $Y_{ni}(z)$ which is directly related to the vertical velocity profile and one can see that Y_{n1} reaches its maximum value near the mid-height of the cylinder while Y_{n2} changes its sign at nearly the same point. Therefore, symmetry with respect to the mid-height of the cylinder is not completely lost when a non-linear equation of state is used. This could explain why the major contribution to $R_{21}^{(i)}$ and $R_{22}^{(i)}$ comes from $i = 2$ like that for ordinary fluids [11]. The behaviour of the term independent of the Prandtl number is quite different since the two contributions $R_{20}^{(1)}$ and $R_{20}^{(2)}$ have opposite sign with $R_{20}^{(1)} < 0$ and $R_{20}^{(2)} > 0$. For $\mu = 1$, $|R_{20}^{(2)}| < R_{20}^{(2)}$ leading to $R_2 > 0$ and thus the bifurcation is supercritical. For $\mu > 1.1$, $|R_{20}^{(1)}| > R_{20}^{(2)}$ and thus

$$R_2 = R_{20} + \frac{1}{\sigma} R_{21} + \frac{1}{\sigma^2} R_{22} \quad (38)$$

with $R_{20} < 0$. This means that for Prandtl numbers such that

$$\sigma > \frac{2R_{22}}{-R_{21} + \sqrt{(R_{21}^2 + 4R_{22}|R_{20}|)}} \quad (39)$$

the bifurcation is subcritical.

Table 4. Numerical values of $R_{20}^{(i)}$, $R_{21}^{(i)}$ and $R_{22}^{(i)}$ for the aspect ratio $\lambda = 2$ and different values of μ

μ	i	$R_{20}^{(i)}$	$R_{21}^{(i)}$	$R_{22}^{(i)}$
1	1	−0.727	0.421	−0.047
	2	1.012	3.018	1.802
	3	−0.013	0.079	0.029
1.1	1	−1.151	0.665	−0.074
	2	1.139	3.265	1.932
	3	0.010	0.145	0.054
1.2	1	−1.829	1.055	−0.119
	2	1.292	3.538	2.062
	3	0.010	0.276	0.099
1.5	1	−7.832	4.522	−0.528
	2	1.509	4.057	2.058
	3	0.253	0.729	0.190

5.2. *Bifurcation at* $\lambda = 3$ *and* 4

Inspection of Tables 5 and 6 shows that most of the remarks valid for $\lambda = 2$ remain qualitatively true for larger aspect ratios. Now the value of μ at which the coefficient R_{20} changes its sign is : $1.20 < \mu < 1.25$ for $\lambda = 3$ and $1.3 < \mu < 1.4$ for $\lambda = 4$. The vertical profiles $Y_{n1}(z)$ are drawn in Fig. 2 for the angular modes $n = 1, 2$. As μ increases from 1 to 2 we observe

Table 5. Numerical values of $R_{20}^{(i)}$, $R_{21}^{(i)}$ and $R_{22}^{(i)}$ for the aspect ratio $\lambda = 3$ and different values of μ

μ	i	$R_{20}^{(i)}$	$R_{21}^{(i)}$	$R_{22}^{(i)}$
1	1	−0.247	0.166	0.012
	2	0.430	1.335	0.614
1.1	1	−0.368	0.242	0.016
	2	0.486	1.397	0.634
1.2	1	−0.540	0.347	0.019
	2	0.547	1.461	0.648
1.25	1	−0.650	0.413	0.020
	2	0.577	1.492	0.653
1.4	1	−1.119	0.682	0.015
	2	0.648	1.589	0.651
2	1	−6.767	3.713	0.353
	2	0.920	3.094	1.001

Table 6. Numerical values of $R_{20}^{(i)}$, $R_{21}^{(i)}$ and $R_{22}^{(i)}$ for the aspect ratio $\lambda = 4$ and different values of μ

μ	i	$R_{20}^{(i)}$	$R_{21}^{(i)}$	$R_{22}^{(i)}$
1	1	−0.166	0.162	0.029
	2	0.311	0.842	0.333
1.2	1	−0.306	0.268	0.042
	2	0.374	0.891	0.341
1.4	1	−0.517	0.407	0.050
	2	0.436	0.985	0.358
1.6	1	−0.824	0.582	0.048
	2	0.503	1.154	0.398
1.8	1	−1.245	0.803	0.034
	2	0.583	1.397	0.466
2.0	1	−1.831	1.102	0.042
	2	0.672	1.691	0.555

that the convection tends to be stronger in the lower part of the cylinder and even for $\mu = 2$ a weak secondary cell appears in the upper part. The presence of a small counter cell has already been quoted in infinite horizontal layers of water when $\mu > 2$ [1, 5, 6].

In the extended horizontal ice–water system, non-linear computations [5] indicate that convection first appears at finite amplitude for a value of the penetration parameter around $\mu = 1.8$. The precise value of μ could be determined as a function of the Prandtl number by the same kind of analysis developed in the present work, allowing a comparison with the carefully controlled experiments carried out in liquid helium [8].

To illustrate our results we have reported in Table 7 the value of R_2 for some values of λ and μ and two particular Prandtl numbers corresponding to water ($\sigma = 7$) and to liquid helium ($\sigma = 0.78$). In the range of values of μ considered ($\mu < 2$) we observe a change of sign of R_2 for all of the aspect ratios $\lambda = 2, 3, 4$ in the case of water. For liquid helium the transition between super- and subcriticality occurs for a higher value of the penetration parameter μ and even for $\lambda = 2, 3$ and $\mu = 2$ it has not been reached.

Table 7. Values of R_2 as a function of λ and μ, for two particular Prandtl numbers corresponding to water ($\sigma = 7$) and liquid helium ($\sigma = 0.78$)

λ	μ	$R_2(H_2O)$	$R_2(^4He)$
2	1.2	0.21	9.07
	1.5	−4.70	8.69
	2.0	−98.26	−14.18
3	1.2	0.31	3.63
	1.4	−0.018	3.98
	2.0	−4.88	3.94
4	1.4	0.18	2.56
	1.6	0.03	2.92
	1.8	−0.205	3.37
	2.0	−0.64	3.26

6. DISCUSSION

The major result of this work is to show that occurrence of subcritical bifurcation is not exclusively caused by the use of a non-linear equation of state as pointed out in ref. [4]. In a cylindrical column of water in the range of temperature where a parabolic equation of state holds, we have shown that the bifurcation is always supercritical when the whole height of water is unstable (no penetrative convection). When there is penetration, the bifurcation can be subcritical if the depth of the stable layer lying above the 4°C isotherm exceeds a certain value which depends upon the aspect ratio of the cylinder. The vanishing of the first coefficient in the expansion of bifurcation parameter (equation (17)) also occurs in the Taylor–Couette problem for which the following term in the expansion has been computed recently in the degenerate case [14]. Azouni [9] reported on the existence of an hysteresis loop associated with an inverted bifurcation for experiments in a cylindrical water layer of aspect ratio $\lambda \approx 4.5$ with the top boundary maintained at 4°C. This result is surprising since in our theoretical model we found a normal bifurcation when the whole height is unstable, in agreement with previous studies in different geometry. This discrepancy can be attributed to the experimental difficulty in establishing a uniform linear temperature gradient along the whole height of a tall cylinder.

Acknowledgements—I am grateful to A. Azouni for communicating her experimental results and for many discussions on the subject.

REFERENCES

1. G. Veronis, Penetrative convection, *Astrophys. J.* **137**, 641–663 (1963).
2. G. P. Merker, P. Waas and U. Grigull, Onset of convection in a horizontal water layer with maximum density effects, *Int. J. Heat Mass Transfer* **22**, 505–515 (1979).
3. B. Gebhart and J. C. Mollendorf, A new density relation for pure and saline water, *Deep Sea Res.* **24**, 831–848 (1977).
4. P. C. Matthews, A model for the onset of penetrative convection, *J. Fluid Mech.* **188**, 571–583 (1988).

5. S. Musman, Penetrative convection, *J. Fluid Mech.* **31**, 343–366 (1968).
6. D. R. Moore and N. O. Weiss, Nonlinear penetrative convection, *J. Fluid Mech.* **61**, 553–581 (1973).
7. A. J. Roberts, An analysis of near-marginal, mildly penetrative convection with heat flux prescribed on the boundaries, *J. Fluid Mech.* **158**, 71–93 (1985).
8. R. W. Walden and G. Ahlers, Non-Boussinesq and penetrative convection in a cylindrical cell, *J. Fluid Mech.* **109**, 89–114 (1981).
9. M. A. Azouni, Hysteresis loop in water between 0 and 4°C, *Geophys. Astrophys. Fluid Dyn.* **24**, 137–142 (1983).
10. M. A. Azouni and C. Normand, Thermoconvective instabilities in a vertical cylinder of water with maximum density effects. Part 2, *Geophys. Astrophys. Fluid Dyn.* **23**, 223–245 (1983).
11. S. Rosenblat, Thermal convection in a vertical circular cylinder, *J. Fluid Mech.* **122**, 395–410 (1982).
12. S. Rosenblat, S. H. Davis and G. M. Homsy, Nonlinear Marangoni convection in bounded layers. Part 1. Circular cylindrical containers, *J. Fluid Mech.* **120**, 91–122 (1982).
13. T. B. Benjamin, Bifurcation phenomena in steady flows of a viscous fluid—I. Theory, *Proc. R. Soc. Lond.* **A359**, 1–26 (1978).
14. P. Laure and Y. Demay, Symbolic computation and equation on the center manifold: application to the Couette–Taylor problem, *Comput. Fluids* **16**, 229–238 (1988).

APPENDIX

Calculation of $\alpha_{n1}^{(i)}$ $(n = 0, 2)$

Setting $x_n = k_n r$ we first establish the following results:

$$(\mathbf{u}_{11}\cdot\nabla)\theta_{11} = \frac{1}{2}[k_1^2 J_1^2(x_1) Y_1 \mathrm{D}X_1 + F_+(x_1) X_1 \mathrm{D}Y_1] + \frac{\cos 2\varphi}{2}[k_1^2 J_1^2(x_1) Y_1 \mathrm{D}X_1 + F_-(x_1) X_1 \mathrm{D}Y_1] \quad \text{(A1)}$$

$$\delta\cdot(\mathbf{u}_{11}\cdot\nabla)\mathbf{u}_{11} = \frac{1}{2}\Delta_0\left[\frac{k_1^2}{2} J_1^2(x_1)\mathrm{D}(Y_1 Z_1) + F_+(x_1) Z_1 \mathrm{D}Y_1\right] + \frac{\cos 2\varphi}{2}\Delta_2\left[\frac{k_1^2}{2} J_1^2(x_1)\mathrm{D}(Y_1 Z_1) + F_-(x_1) Z_1 \mathrm{D}Y_1\right] \quad \text{(A2)}$$

where we have introduced the following notations:

$$Z_n = (\mathrm{D}^2 - k_n^2) Y_n \quad \text{(A3)}$$

$$F\pm(x_1) = \left|\frac{\partial J_1(x_1)}{\partial r}\right|^2 \pm \frac{J_1^2(x_1)}{r^2} \quad \text{(A4)}$$

$$\Delta_n = \frac{1}{r}\frac{\partial}{\partial r} r \frac{\partial}{\partial r} - \frac{n^2}{r^2}. \quad \text{(A5)}$$

After multiplying equation (A1) by θ_{ni}^* and equation (A2) by ϕ_{ni}^* and integrating over the volume of the cylinder one sees that integration over the radial variable involves two elementary integrals

$$a_n = \int_0^1 J_n(k_n r) J_1^2(k_1 r) r\,\mathrm{d}r, \quad n = 0, 2. \quad \text{(A6)}$$

After addition of the contributions from equations (A1) and (A2) the quantity $\alpha_{n1}^{(i)}$ defined in equation (30) becomes

$$\alpha_{n1}^{(i)} = -\frac{a_n}{2}\left\{\left[k_1^2 \overline{X_1 Y_1 \mathrm{D}X_{ni}^*} + \frac{k_n^2}{2}\overline{X_1 \mathrm{D}Y_1 X_{ni}^*}\right] + \frac{k_n^2}{\sigma}\left[\frac{k_1^2}{2}\overline{Y_1 Z_1 \mathrm{D}Y_{ni}^*} - \left(k_1^2 - \frac{k_n^2}{2}\right)\overline{Z_1 \mathrm{D}Y_1 Y_{ni}^*}\right]\right\} \quad \text{(A7)}$$

where the overbar means integration over the vertical variable.

Calculation of $\alpha_n^{(i)}$

At third order in ε the resonance terms in heat advection are

$$(\mathbf{u}_{11}\cdot\nabla)\theta_{ni} + (\mathbf{u}_{ni}\cdot\nabla)\theta_{11} = \frac{2}{2+n}\cos\varphi[J_1(x_1)J_n(x_n)(k_1^2 Y_1 \mathrm{D}X_{ni} + k_n^2 Y_{ni}\mathrm{D}X_1) + F_{1n}(r)(X_{ni}\mathrm{D}Y_1 + X_1\mathrm{D}Y_{ni})] \quad \text{(A8)}$$

where we have introduced the following notations:

$$F_{10}(r) = \frac{\partial J_1(x_1)}{\partial r}\frac{\partial J_0(x_0)}{\partial r} \quad \text{(A9)}$$

$$F_{12}(r) = \frac{\partial J_1(x_1)}{\partial r}\frac{\partial J_2(x_2)}{\partial r} + 2\frac{J_1(x_1)J_2(x_2)}{r^2}. \quad \text{(A10)}$$

The resonant terms in momentum advection are

$$\delta\cdot[(\mathbf{u}_{11}\cdot\nabla)\mathbf{u}_{ni} + (\mathbf{u}_{ni}\cdot\nabla)\mathbf{u}_{11}] = \frac{2}{2+n}\cos\varphi\{k_1^2 k_n^2[\mathrm{D}(Y_1 Y_{ni})\Delta_1(J_1(x_1)J_n(x_n)) + \mathrm{D}(Y_1 Y_{ni}'' + Y_1'' Y_{ni}) J_1(x_1)J_n(x_n)] - F_{1n}(r)[k_1^2\mathrm{D}(Y_1 Y_{ni}'') + k_n^2\mathrm{D}(Y_1'' Y_{ni})] - (Z_1\mathrm{D}Y_{ni} + Z_{ni}\mathrm{D}Y_1)\Delta_1 F_{1n}(r)\}. \quad \text{(A11)}$$

After multiplying equation (A8) by θ_{11}^* and equation (A11) by ϕ_{11}^* and integrating over the volume of the cylinder one obtains

$$\alpha_n^{(i)} = \frac{2a_n}{2+n}\left\{\left[k_1^2\overline{X_1^* Y_1 \mathrm{D}X_{ni}} + \frac{k_n^2}{2}(\overline{X_1 \mathrm{D}Y_1^* X_{ni}} + \overline{Y_{ni}(X_1^*\mathrm{D}X_1 - X_1\mathrm{D}X_1^*)})\right] + \frac{k_n^2}{\sigma}\left[\frac{k_1^2}{2}(\overline{Y_1^* Z_1 \mathrm{D}Y_{ni}} + \overline{Z_{ni}(Y_1^*\mathrm{D}Y_1 - Y_1\mathrm{D}Y_1^*)}) - \left(k_1^2 - \frac{k_n^2}{2}\right)\overline{Z_1 \mathrm{D}Y_1^* Y_{ni}}\right]\right\}. \quad \text{(A12)}$$

Comparison of expressions (A7) and (A12) shows that when the linear differential system is selfadjoint the quantities $\alpha_{ni}^{(i)}$ and $\alpha_n^{(i)}$ have opposite sign.

TRANSITION ENTRE BIFURCATION SUPERCRITIQUE ET SOUSCRITIQUE EN CONVECTION PENETRANTE DANS UN CYLINDRE VERTICAL

Résumé—On considère la stabilité d'une colonne d'eau dans un cylindre vertical lorsque la temperature à la base du cylindre est maintenue à 0°C et la temperature au sommet varie entre 4 et 8°C. L'analyse de la transition vers le regime convectif faiblement non linéaire montre que la bifurcation est soit supercritique soit sous-critique selon les valeurs prises par deux parametres: le rapport d'aspect du cylindre (hauteur/rayon) qui varie de 2 à 4, et le paramètre de pénétration μ défini comme le rapport de la hauteur totale de fluide à la hauteur de l'isotherme 4°C. Pour une valeur donnée du rapport d'aspect, la bifurcation est super-critique lorsque toute la colonne est instable ($\mu = 1$) et devient sous-critique au-dessus d'une certaine valeur de μ lorsqu'il y a pénétration ($\mu > 1$).

ÜBERGANG VON UNTERKRITISCHER ZU ÜBERKRITISCHER GABELSTRÖMUNG BEI DER KONVEKTION IN EINEM SENKRECHTEN ZYLINDER

Zusammenfassung—Es wird die Stabilität einer senkrechten zylindrischen Wassersäule untersucht, deren waagerechte untere Stirnfläche auf 0°C gehalten wird, während die Temperatur der oberen Stirnfläche zwischen 4 und 8°C variiert. Eine leicht nichtlineare analytische Untersuchung zeigt, daß die Gabelströmung entweder überkritisch oder unterkritisch ist—abhängig von zwei Parametern: dem Seitenverhältnis des Zylinders (Höhe/Radius), das zwischen 2 und 4 liegt, und dem Eindringparameter μ, der als das Verhältnis der gesamten Höhe zur Höhe der 4°C-Isothermen definiert ist. Für einen vorgegebenen Wert des Seitenverhältnisses ist die Gabelströmung überkritisch, wenn die gesamte Höhe instabil ist ($\mu = 1$), sie wird unterkritisch oberhalb eines ganz bestimmten Wertes von μ, wenn $\mu > 1$ wird.

ПЕРЕХОД ОТ ДОКРИТИЧЕСКОЙ К ЗАКРИТИЧЕСКОЙ БИФУРКАЦИИ ПРИ ПРОНИКАЮЩЕЙ КОНВЕКЦИИ В ВЕРТИКАЛЬНОМ ЦИЛИНДРЕ

Аннотация—Исследуется конвективная устойчивость вертикального цилиндрического водяного столба, на нижней границе которого поддерживается температура 0°C, а на верхней она изменяется от 4 до 8°C. Анализ с учетом слабой нелинейности показывает, что бифуркация начинается либо в закритической, либо в докритической области в зависимости от значений двух параметров: отношения высоты цилиндра к его радиусу, изменяющегося в пределах от 2 до 4, а также параметра проникновения μ, определямого как отношение высоты цилиндра к высоте, на которой располагается изотерма, соответствующая 4°C. Для заданного значения отношения высоты к радиусу бифуркация начинается в закритической области, когда жидкость по всей высоте теряет устойчивость ($\mu = 1$), и становится докритическим, когда происходит процесс проникновения возмущений в неподвижную жидкость ($\mu > 1$).